16th World Conference on Earthquake, 16WCEE 2017

Santiago Chile, January 9th to 13th 2017

Paper N° 4596

Registration Code: S-H1464736190

SEISMIC PROTECTION OF ADJACENT BASE-ISOLATED BUILDINGS USING THE CONNECTED CONTROL METHOD

S. Lobo[1], R. Christenson[2], P. Brewick[3], E. Johnson[4]

[1] *Ph.D. student, Department of Civil and Environmental Engineering, University of Connecticut, USA, sergio.la@engr.uconn.edu.*

[2] *Professor, Department of Civil and Environmental Engineering, University of Connecticut, USA, rchriste@engr.uconn.edu.*

[3] *Postdoctoral Researcher, Dept. of Civil and Environmental Engineering, University of Southern California, USA, brewick@usc.edu.*

[4] *Professor, Department of Civil and Environmental Engineering, University of Southern California, USA, JohnsonE@usc.edu*

Abstract

Seismic isolation is a popular type of seismic protective system in which the dominant resonant frequencies of the structure are moved to the lower frequency range of the spectrum to protect the structure and its contents from ground accelerations. Isolating the structure is an effective way to attenuate vibration of the superstructure when subjected to earthquakes with significantly higher dominant frequencies, but at the same time this approach increases the vulnerability of the structure to long-period long-duration earthquakes. This paper proposes the application of the connected control method to provide isolation performance for long-period long-duration earthquakes without compromising the isolation at higher frequencies. An analytical model is presented to demonstrate through a frequency domain analysis that the connected control method can be applied to adjacent base isolated buildings to provide reduction in the isolator resonant peaks while not increasing the attenuation of the responses, thus protecting the isolated buildings from long-period long-duration earthquakes without affecting the performance of the isolation to higher frequency excitation.

Keywords: base isolation; connected control method

1. Introduction

Seismic protection techniques mitigate the negative effects of earthquakes on structures. In the case of buildings, the conventional structural design method provides sufficient strength and energy dissipation capacity through the utilization of proper materials and structural configurations, as well as exhaustive detailing. This methodology offers adequate solutions when the required performance objectives allow for the occurrence of either structural damage during larger design level earthquakes or non-structural damage for less intense earthquakes. However, there are cases where it is desired that structures remain fully operational (limited structural and non-structural damage) immediately following the occurrence of the design earthquake. For example, hospitals and disaster mitigation facilities are expected to operate immediately after the occurrence of a strong shaking. Furthermore, in some cases, it may not be practical to provide sufficient resistance or ductility. For example, seismic retrofit of existing buildings might be very sensitive to disturbances and, therefore, require minimal interventions. As such, techniques such as base isolation have been used in the past and are increasingly considered as a practical alternative for the seismic protection of buildings.

Based-isolated buildings are effective to reduce the response of buildings when subjected to ground excitation with frequency content well above the natural frequency of the isolation layer. However, base isolation may be less effective, and even induce negative effects, when base-isolated structures are subjected to long-period, long-duration earthquakes, such as the events of Mexico City in 1985 and, more recently, Tohoku in 2011. This is a result of frequencies that can excite the natural frequency of the isolated structure over durations long enough for amplitudes to increase beyond the capacity of the isolators and isolation system. One approach to address this concern is to increase the damping in the isolation layer, though this reduces the level of isolation that can be achieved at higher frequencies.

The connected control method is another seismic protection technology that has been proposed for adjacent fixed-base structures (Klein et al. 1972, Kunieda 1976 and Seto 1994). In this technique, adjacent buildings are connected together with stiffness, damping and/or actuation devices to allow the multiple buildings to work in unison to absorb and dissipate the energy of the earthquake. Coupling buildings has been realized on actual buildings in Japan.

This paper explores the effectiveness of applying the connected control method to adjacent based-isolated buildings subjected to long-period, long-duration earthquakes. The first section presents the idealized system and the methodology used to evaluate the effectiveness of the proposed strategy. Next, results are presented and discussed. Finally, conclusions on the effectiveness of the connected control method on base isolated buildings are drawn.

2. Maintained Isolation of Connected Control Method

Consider a damped single-degree-of-freedom system (SDOF), with mass m, stiffness k and damping coefficient c, that is allowed to displace along direction x and is subjected to a ground acceleration $\ddot{x}_{\mathrm{g}}$. The equation of motion for such a system is

$$m\ddot{x} + c\dot{x} + kx = -m\ddot{x}_{\mathrm{g}} \tag{1}$$

The frequency response function (FRF) of the mass displacement to ground acceleration can be shown to be

$$D(\omega) = \frac{-1}{-\omega^2 + 2\xi\omega_{\mathrm{n}} j\omega + \omega_{\mathrm{n}}{}^2} \tag{2}$$

where ω_{n} is the natural frequency, ξ is the damping ratio and ω is the frequency. The corresponding FRF of the absolute acceleration of the mass to the ground acceleration can be shown to be:

$$A(\omega) = \frac{2\xi\omega_{\mathrm{n}} j\omega + \omega_{\mathrm{n}}^2}{-\omega^2 + 2\xi\omega_{\mathrm{n}} j\omega + \omega_{\mathrm{n}}^2} \tag{3}$$

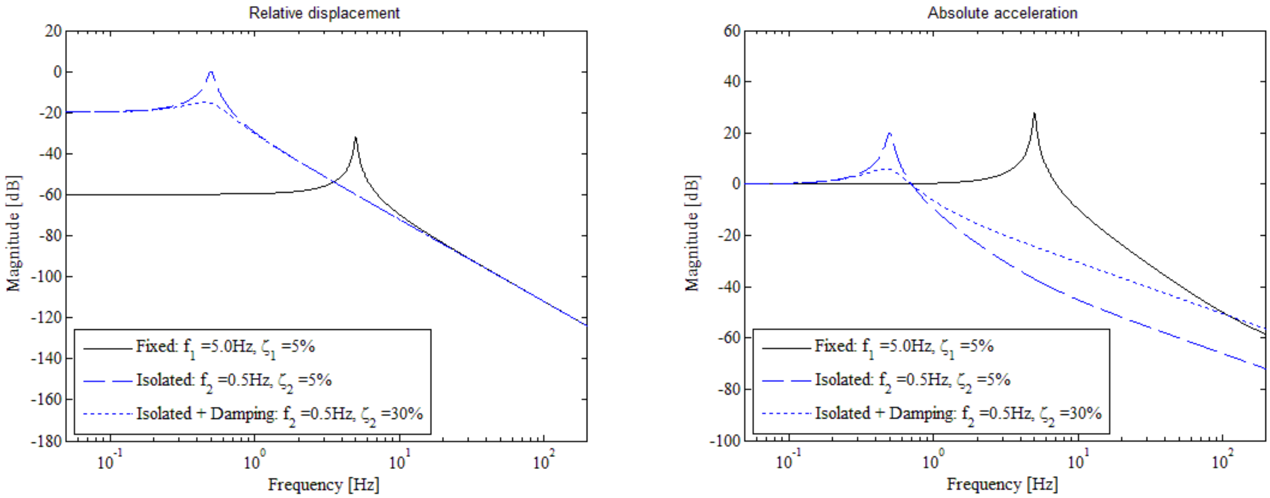

Fig. 1 – Frequency response functions for a SDOF system.

Figure 1 shows the magnitude of the FRFs in equations Eqs. (2)–(3) for two different natural frequency and damping ratios. Decreasing the natural frequency, as is done when base-isolating a structure, decreases the resonance of the displacement, effectively moving the resonance below the frequency range of typical earthquakes. For long-period earthquakes, the energy can approach the isolated resonance. In this case, for displacement protection it is necessary to reduce the resonant peak. This can be done by increasing the damping. Increasing the damping is observed to have little effect on the higher frequency displacement magnitude; however, increasing the damping increases the magnitude of the acceleration FRF at higher frequencies, which can negate the benefit of the isolation for the acceleration-dependent nonstructural components needed for the building to remain fully operational. The method presented in this paper rather explores an alternative in which dampers are located at the superstructure level between adjacent base-isolated buildings, i.e., combining base isolation with the connected control method (CCM).

To better understand the benefit of the connected control method, first consider two SDOF systems, buildings A and B, coupled with a viscous damping element. To simplify this analysis, it is assumed that the building models are undamped. The equations of motion for this two SDOF are:

$$m_\mathrm{a}\ddot{x}_\mathrm{a} + c(\dot{x}_\mathrm{ac} - \dot{x}_\mathrm{bc}) + k_\mathrm{a}x_\mathrm{ac} = -m_\mathrm{a}\ddot{x}_\mathrm{g} \tag{4}$$

$$m_\mathrm{b}\ddot{x}_\mathrm{b} + c(\dot{x}_\mathrm{bc} - \dot{x}_\mathrm{ac}) + k_\mathrm{b}x_\mathrm{bc} = -m_\mathrm{b}\ddot{x}_\mathrm{g} \tag{5}$$

where x_ac and x_bc indicate the displacements of buildings A and B, respectively, when they are coupled together. As for the SDOF system in Eq. (1), Eqs. (4)–(5) can be transformed into the Laplace domain. In order to solve this system of equations, they can be grouped in matrix form as:

$$\begin{bmatrix} s^2 + \frac{c}{m_\mathrm{a}}s + \omega_\mathrm{a}^2 & -\frac{c}{m_\mathrm{a}}s \\ -\frac{c}{m_\mathrm{b}}s & s^2 + \frac{c}{m_\mathrm{b}}s + \omega_\mathrm{b}^2 \end{bmatrix} \begin{bmatrix} X_\mathrm{ac}(s) \\ X_\mathrm{bc}(s) \end{bmatrix} = \begin{bmatrix} -\ddot{X}_\mathrm{g}(s) \\ -\ddot{X}_\mathrm{g}(s) \end{bmatrix} \tag{6}$$

The off-diagonal elements of this matrix are the mathematical representation of the physical coupling of these two structures. Application of Cramer's rule in Eq. (6) provides the solution for the relative displacement of building A, which is represented by

$$X_\mathrm{ac}(s) = \frac{\begin{vmatrix} -\ddot{X}_\mathrm{g} & -\frac{c}{m_\mathrm{a}}s \\ -\ddot{X}_\mathrm{g} & s^2+\frac{c}{m_\mathrm{b}}s+\omega_\mathrm{b}^2 \end{vmatrix}}{\begin{vmatrix} s^2+\frac{c}{m_\mathrm{a}}s+\omega_\mathrm{a}^2 & -\frac{c}{m_\mathrm{a}}s \\ -\frac{c}{m_\mathrm{b}}s & s^2+\frac{c}{m_\mathrm{b}}s+\omega_\mathrm{b}^2 \end{vmatrix}} = \frac{\left(-s^2-\frac{c}{m_\mathrm{b}}s-\omega_\mathrm{b}^2-\frac{c}{m_\mathrm{a}}s\right)}{\left(s^2+\frac{c}{m_\mathrm{a}}s+\omega_\mathrm{a}^2\right)\left(s^2+\frac{c}{m_\mathrm{b}}s+\omega_b^2\right)-\frac{c^2}{m_\mathrm{a}m_\mathrm{b}}s^2}\ddot{X}_\mathrm{g}(s) \tag{7}$$

Then, the transfer function for the relative displacement is expressed as

$$D_{\mathrm{ac}}(s)=\frac{X_{\mathrm{ac}}(s)}{\ddot{X}_{\mathrm{g}}(s)}=\frac{-s^2-\left(\frac{m_{\mathrm{a}}+m_{\mathrm{b}}}{m_{\mathrm{a}}m_{\mathrm{b}}}\right)cs-\omega_{\mathrm{b}}^2}{s^4+\left(\frac{m_{\mathrm{a}}+m_{\mathrm{b}}}{m_{\mathrm{a}}m_{\mathrm{b}}}\right)cs^3+(\omega_{\mathrm{a}}^2+\omega_{\mathrm{b}}^2)s^2+\left(\frac{m_{\mathrm{a}}\omega_{\mathrm{a}}^2+m_{\mathrm{b}}\omega_{\mathrm{b}}^2}{m_{\mathrm{a}}m_{\mathrm{b}}}\right)cs+(\omega_{\mathrm{a}}^2\omega_{\mathrm{b}}^2)} \tag{8}$$

It should be noted that when $c=0$, the expression for building A reverts back to the SDOF system in Eqs. (1)–(2). In order to calculate the magnitude of Eq. (8), it is convenient to rearrange the expression as

$$D_{\mathrm{ac}}(j\omega)=\frac{[\omega^2-\alpha\omega_{\mathrm{a}}^2]+[-\beta\gamma\omega]j}{[(\omega^2-\alpha\omega_{\mathrm{a}}^2)(\omega^2-\omega_{\mathrm{a}}^2)]+[-\beta\gamma\omega^3+\delta\gamma\omega_{\mathrm{a}}^2\omega]j} \tag{9}$$

where

$$\alpha=\ \omega_{\mathrm{b}}^2/\omega_{\mathrm{a}}^2 \tag{10}$$
$$\beta=(m_{\mathrm{a}}+m_{\mathrm{b}})/m_{\mathrm{b}} \tag{11}$$
$$\gamma=c/m_{\mathrm{a}} \tag{12}$$
$$\delta=\left(m_{\mathrm{a}}\omega_{\mathrm{a}}^2+m_{\mathrm{b}}\omega_{\mathrm{b}}^2\right)/m_{\mathrm{b}} \tag{13}$$

It is noteworthy to mention that damping is present in the imaginary terms only, which is consistent with basic dynamic theory. The magnitude of $D_{\mathrm{ac}}(\omega)$ is given by

$$d_{\mathrm{ac}}(j\omega)=\sqrt{\frac{[\omega^2-\alpha\omega_{\mathrm{a}}^2]^2+[(\beta)(\gamma\omega)]^2}{[(\omega^2-\alpha\omega_{\mathrm{a}}^2)(\omega^2-\omega_{\mathrm{a}}^2)]^2+[(-\beta\omega^2+\delta\omega_{\mathrm{a}}^2)(\gamma\omega)]^2}} \tag{14}$$

For the case of absolute accelerations, a similar procedure is used to obtain

$$A_{\mathrm{ac}}(j\omega)=-\omega_{\mathrm{a}}^2D_{\mathrm{ac}}(j\omega) \tag{15}$$

and the corresponding magnitude can be shown to be

$$a_{\mathrm{ac}}(j\omega)=\omega_{\mathrm{a}}^2d_{\mathrm{ac}}(j\omega) \tag{16}$$

Following a similar procedure, the following expression is obtained for building B

$$D_{\mathrm{bc}}(j\omega)=\frac{[\omega^2-\omega_{\mathrm{a}}^2]+[-\beta\gamma\omega]j}{[(\omega^2-\alpha\omega_{\mathrm{a}}^2)(\omega^2-\omega_{\mathrm{a}}^2)]+[-\beta\gamma\omega^3+\delta\gamma\omega_{\mathrm{a}}^2\omega]j} \tag{17}$$

The magnitude of displacement for building B is

$$d_{\mathrm{bc}}(j\omega)=\sqrt{\frac{[\omega^2-\omega_{\mathrm{a}}^2]^2+[(\beta)(\gamma\omega)]^2}{[(\omega^2-\alpha\omega_{\mathrm{a}}^2)(\omega^2-\omega_{\mathrm{a}}^2)]^2+[(-\beta\omega^2+\delta\omega_{\mathrm{a}}^2)(\gamma\omega)]^2}} \tag{18}$$

Finally, the FRF for absolute acceleration building B is

$$A_{\mathrm{bc}}(j\omega)=-\omega_{\mathrm{a}}^2D_{\mathrm{bc}}(j\omega) \tag{19}$$
$$a_{\mathrm{bc}}(j\omega)=\omega_{\mathrm{a}}^2d_{\mathrm{bc}}(j\omega) \tag{20}$$

For the coupled building it was shown that $A_{\mathrm{ac}}(j\omega)=-\omega_{\mathrm{a}}^2D_{\mathrm{ac}}(j\omega)$. Therefore

$$a_{\mathrm{ac}}(j\omega) = \omega_{\mathrm{a}}^2 d_{\mathrm{ac}}(j\omega) = \omega_{\mathrm{a}}^2 \sqrt{\frac{[\omega^2-\alpha\omega_{\mathrm{a}}^2]^2+[(\beta)(\gamma\omega)]^2}{[(\omega^2-\alpha\omega_{\mathrm{a}}^2)(\omega^2-\omega_{\mathrm{a}}^2)]^2+[(-\beta\omega^2+\delta\omega_{\mathrm{a}}^2)(\gamma\omega)]^2}} \quad (21)$$

Considering frequencies significantly larger than the natural frequency ω_{a}, the terms associated with the natural frequencies are small compared to the exciting frequencies and the following expression is obtained

$$a_{\mathrm{ac}}(j\omega) \approx \omega_{\mathrm{a}}^2 \sqrt{\frac{\omega^4+\beta^2\gamma^2\omega^2}{\omega^8+\beta^2\gamma^2\omega^6}} = \omega_{\mathrm{a}}^2 \sqrt{\frac{\omega^2(\omega^2+\beta^2\gamma^2)}{\omega^6(\omega^2+\beta^2\gamma^2)}} = \frac{\omega_{\mathrm{a}}^2}{\omega^2} \quad (22)$$

From Eq. (22), it is observed that, as the isolation frequency is decreased, so is the magnitude of the absolute acceleration FRF. More importantly, Eq. (22) shows that the magnitude at frequencies sufficiently larger than the isolation frequency are independent of the coupling damping c. That is to say that at high frequencies, the magnitude of the absolute acceleration FRF to a ground acceleration coupled with a damping element, c, approaches the same magnitude as the system with $c = 0$.

Figure 2 shows the magnitude of the FRFs in Eqs. (14), (16), (18) and (20) for the connected and unconnected systems. Adding damping in the connected control method is observed to decrease the magnitude of the resonant peaks of the FRFs; however, importantly it does not increase the magnitude of the FRFs for displacement and acceleration in both buildings at higher frequencies, as indicated in Eq. (22). This figure illustrates the benefit of the CCM for adjacent base isolated structures.

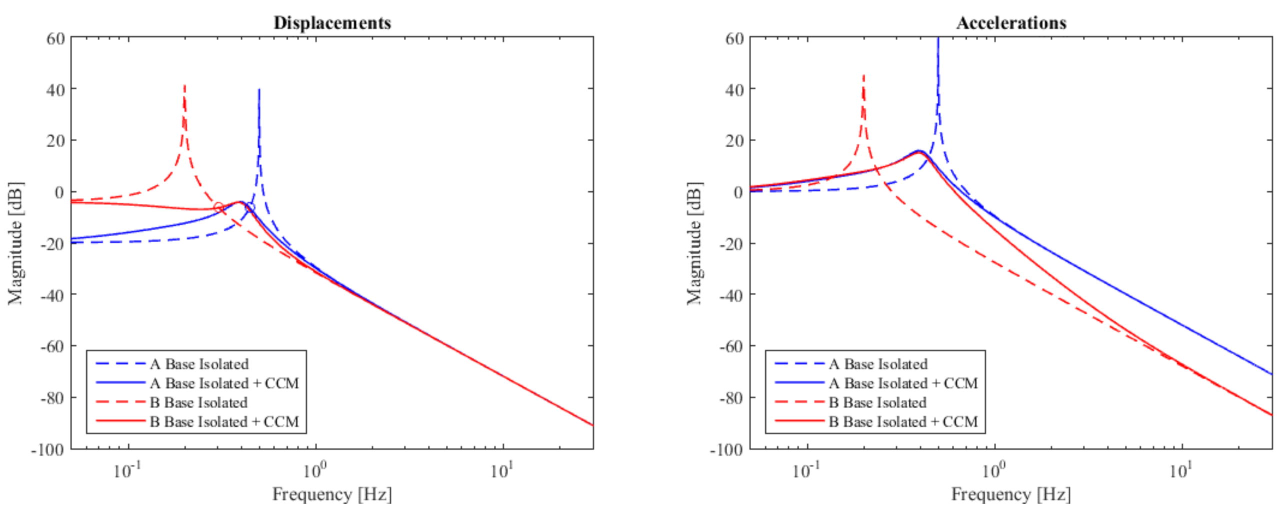

Fig. 2 – Frequency response functions for the coupled SDOF systems.

3. Connected Control Method for Base Isolation Example

This section provides a numerical example to illustrate the benefits of applying the connected control method for adjacent base isolated buildings for seismic protection, as shown in Fig. 3. The buildings are modeled as two-degrees-of freedom systems with lumped masses with identical fixed based properties of 2 Hz natural frequencies and 2% critical damping ratios, where the mass (m), stiffness (k) and damping coefficient (c) of the superstructure are used to determine these quantities. The mass m_{b} of the isolation layer is one third of the mass m of the superstructure. The isolation layer provides an isolated natural frequency of 0.5 Hz for the first structure and 0.2 Hz for the second structure, with identical damping in the isolation layer at 10% of critical. The mass of the isolation layer and superstructure ($m + m_{\mathrm{b}}$), the stiffness of the isolation layer (k_{bi}) and damping of the isolation layer (c_{bi}) are used to determine the dynamic characteristics. The damping coefficient of the connector between the two superstructures is c_{c} and the stiffness between the two structures is k_{c}. The properties of the two structures are summarized in Table 1.

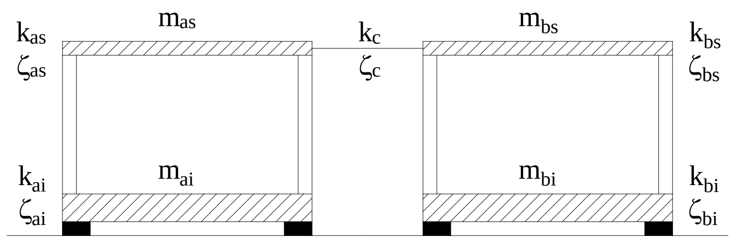

Fig. 3 – Two undamped SDOF systems connected by a damper and spring element

Table 1 – Physical Properties of Adjacent Base Isolated Buildings

	Building A	Building B
Superstructure		
Mass	1 kg	1 kg
Period	0.2 sec	0.2 sec
Damping Ratio	2%	2%
Isolation Layer		
Mass	1/3 kg	1/3 kg
Period*	2 sec	5 sec
Damping Ratio*	10%	10%

* Dynamic characteristics determined assuming the mass of the superstructure is lumped onto the mass of the isolation layer.

The equations of motion for these isolated structures can be represented in matrix form as:

$$\begin{aligned} &\underline{m}\cdot\underline{\ddot{x}}+\underline{c}\cdot\underline{\dot{x}}+\underline{k}\cdot\underline{x}=-\underline{m}\cdot\underline{\Gamma_g}\cdot\ddot{x}_g \\ &\underline{\ddot{x}}=-\underline{m^{-1}}\cdot\underline{k}\cdot\underline{x}-\underline{m^{-1}}\cdot\underline{c}\cdot\underline{\underline{\dot{x}}}-\underline{m^{-1}}\cdot\underline{m}\cdot\underline{\Gamma_g}\cdot\ddot{x}_g \\ &\quad=-\underline{m^{-1}}\cdot\underline{k}\cdot\underline{x}-\underline{m^{-1}}\cdot\underline{c}\cdot\underline{\dot{x}}-\underline{\Gamma_g}\cdot\ddot{x}_g \end{aligned} \tag{23}$$

where the displacements, velocities and accelerations of the isolation layers and the superstructures relative to the ground are defined as $\underline{x}=[x_{ai}\quad x_{as}\quad x_{bs}\quad x_{bi}]^T$, $\underline{\dot{x}}=[\dot{x}_{ai}\quad \dot{x}_{as}\quad \dot{x}_{bs}\quad \dot{x}_{bi}]^T$, and $\underline{\ddot{x}}=[\ddot{x}_{ai}\quad \ddot{x}_{as}\quad \ddot{x}_{bs}\quad \ddot{x}_{bi}]^T$ and the mass, stiffness and mass are defined as

$$\underline{m}=\begin{bmatrix} m_{ai} & 0 & 0 & 0 \\ 0 & m_{as} & 0 & 0 \\ 0 & 0 & m_{bs} & 0 \\ 0 & 0 & 0 & m_{bi} \end{bmatrix}$$

$$\underline{k}=\begin{bmatrix} k_{ai}+k_{as} & -k_{as} & 0 & 0 \\ k_{as} & k_{as}+k_c & -k_c & 0 \\ 0 & -k_c & k_{bs}+k_c & -k_c \\ 0 & 0 & -k_c & k_{ai}+k_{as} \end{bmatrix}$$

$$\underline{c}=\begin{bmatrix} c_{ai}+c_{as} & -c_{as} & 0 & 0 \\ c_{as} & c_{as}+c_c & -c_c & 0 \\ 0 & -c_c & c_{bs}+c_c & -c_c \\ 0 & 0 & -c_c & c_{ai}+c_{as} \end{bmatrix}$$

The loading vector $\underline{\Gamma}_{\mathrm{g}}$ defines the loading of the ground acceleration onto the structure. The state-space representation of the system is

$$\begin{aligned}\dot{\underline{Z}} &= \underline{A}\cdot\underline{Z} + \underline{B}\cdot\underline{U} \\ \underline{Y} &= \underline{C}\cdot\underline{Z} + \underline{D}\cdot\underline{U}\end{aligned} \tag{24}$$

where the states are defined as $\underline{Z} = \begin{bmatrix}\underline{x}^{\mathrm{T}} & \dot{\underline{x}}^{\mathrm{T}}\end{bmatrix}^{\mathrm{T}}$ and $\dot{\underline{Z}} = \begin{bmatrix}\dot{\underline{x}}^{\mathrm{T}} & \ddot{\underline{x}}^{\mathrm{T}}\end{bmatrix}^{\mathrm{T}}$, the input is $\underline{U} = \underline{\Gamma}_{\mathrm{g}}\ddot{x}_{\mathrm{g}}$ and the output is defined as $\underline{Y} = \begin{bmatrix}\underline{x}^{\mathrm{T}} & \dot{\underline{x}}^{\mathrm{T}} & \ddot{\underline{x}}^{\mathrm{T}} + \underline{1}^{\mathrm{T}}\ddot{x}_{\mathrm{g}}\end{bmatrix}^{\mathrm{T}}$. The state space matrices of this representation are given as:

$$\underline{A} = \begin{bmatrix}\underline{0} & \underline{1} \\ -\underline{m}^{-1}\underline{k} & -\underline{m}^{-1}\underline{c}\end{bmatrix}, \quad \underline{B} = \begin{bmatrix}\underline{0} \\ \underline{1}\end{bmatrix},$$
$$\underline{C} = \begin{bmatrix}\underline{1} & \underline{0} \\ \underline{0} & \underline{1} \\ -\underline{m}^{-1}\underline{k} & -\underline{m}^{-1}\underline{c}\end{bmatrix}, \quad \underline{D} = \begin{bmatrix}\underline{0} \\ \underline{0} \\ \underline{0}\end{bmatrix},$$

where $\underline{0}$ and $\underline{1}$ are matrices or vectors of appropriate sizes. To select the optimal values for the stiffness and damping of the connector link, a parameter search is conducted. Figures 4 and 5 show the contour plots for the maximum FRF magnitude for the displacement and absolute acceleration FRFs. The FRFs are determined from the state space model of the system using MATLAB.

The optimal values for connector stiffness and damping are selected as $k_{\mathrm{c}} = 0.90$ and $c_{\mathrm{c}} = 2.45$ to provide a balance of response reduction between both buildings. The resulting FRFs for the structure as fixed base, base isolated, base isolated with damping added to the isolation layer, and CCM base isolated are shown in Figs. 6–7.

The absolute acceleration response is considered here with the performance objective to keep the buildings fully operational immediately following the occurrence of the design earthquake by ensuring the acceleration responses are minimized. The absolute acceleration frequency response functions of the two base isolated buildings are shown in Figure 7 for the four cases. It is observed in this figure that adding the isolation layer reduces the resonant peak of the 5 Hz fixed-base structures to 0.5 Hz and 0.2 Hz for isolated building A and isolated building B, respectively. It is also noted that providing isolation reduces the acceleration responses by an order of magnitude (20 dB) above 1 Hz, which demonstrates the benefits of isolation. The magnitude of the resonant peaks, however, has increased from 28 dB for the fixed base structures to 34 dB for the isolated structures. This 6 dB increase corresponds to an increase by a factor of 2. This can be significant if, during a long-period long-duration earthquake, the resonance is excited.

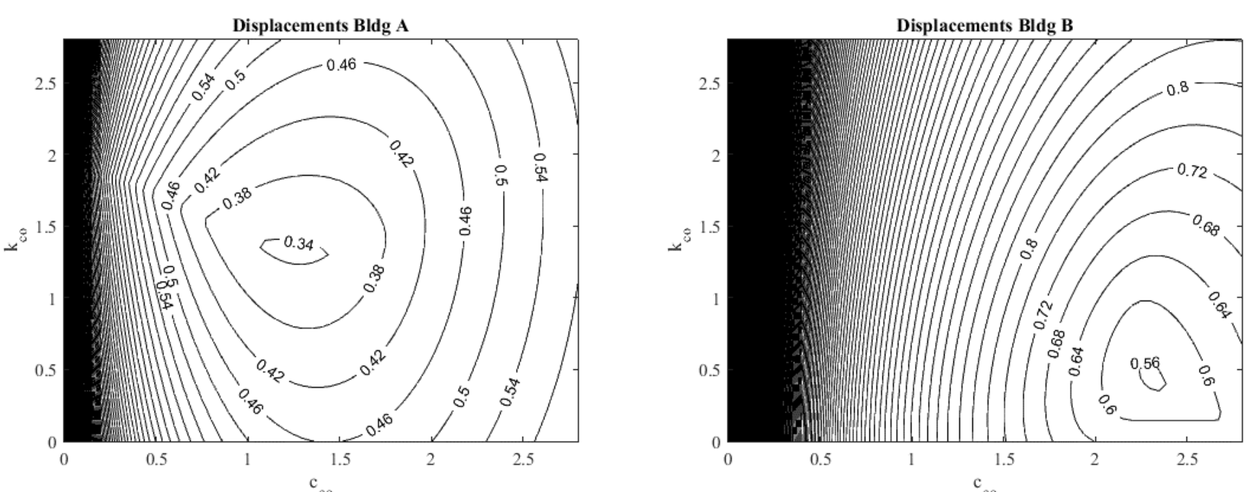

Fig. 4 – Contour plots for maximum displacement FRF.

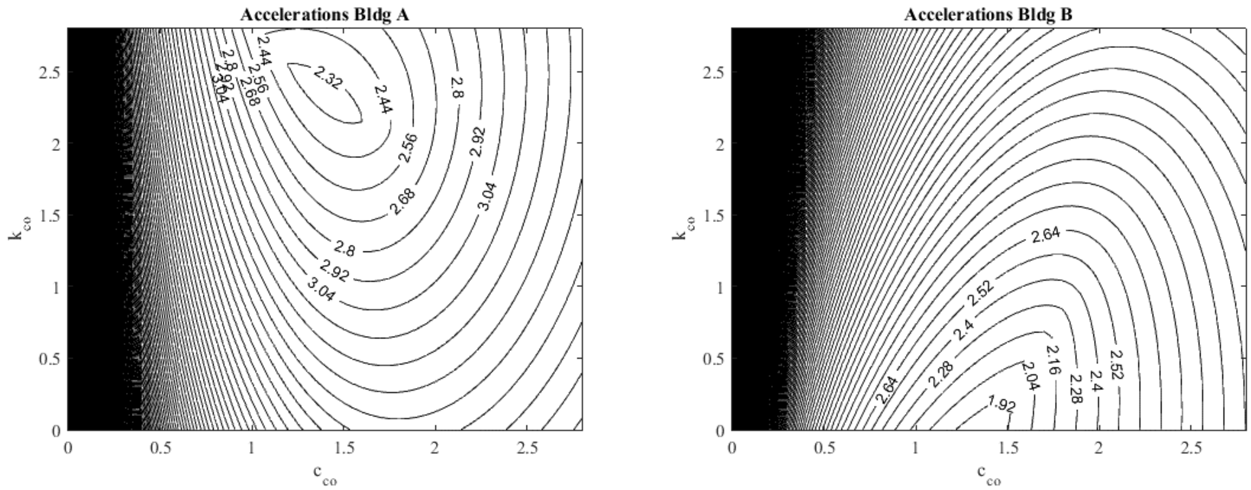

Fig. 5 – Contour plots for maximum absolute acceleration FRF.

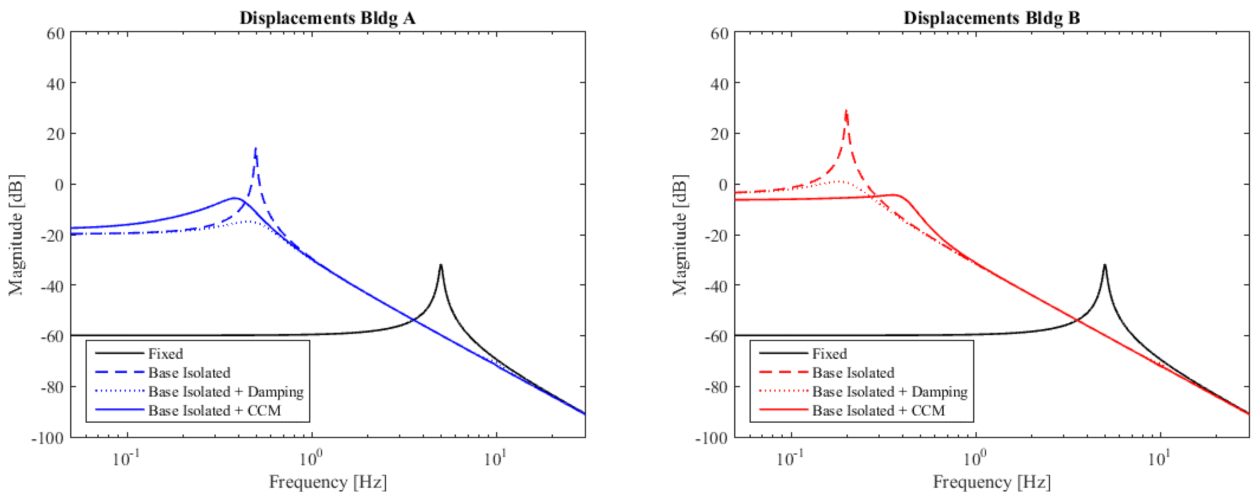

Fig. 6 – Displacement FRF of CCM Base Isolated Buildings.

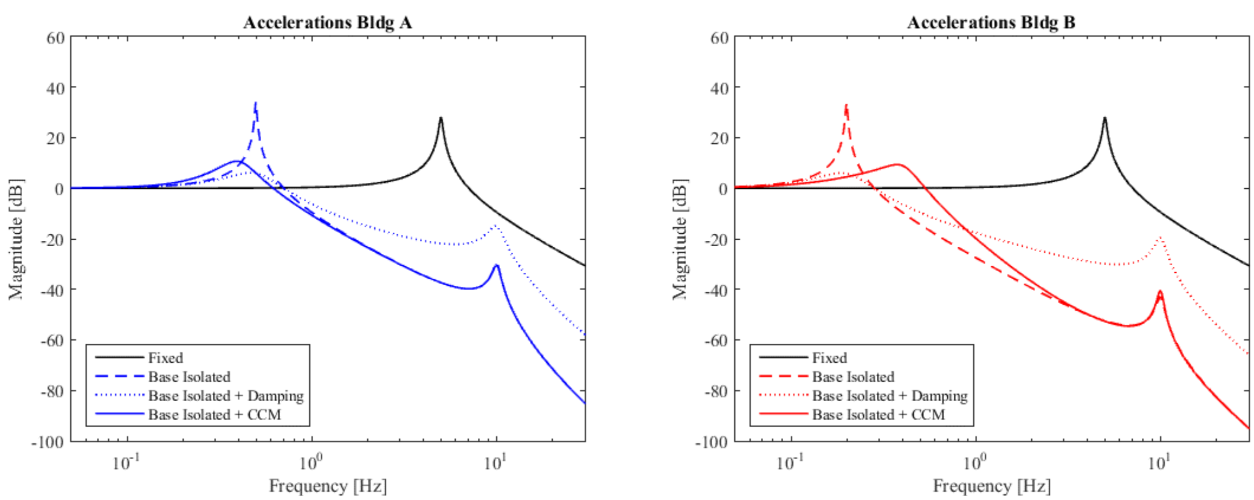

Fig. 7 – Absolute Acceleration FRF of CCM Base Isolated Buildings.

The absolute acceleration response is considered here with the performance objective to keep the buildings fully operational immediately following the occurrence of the design earthquake by ensuring the acceleration responses are minimized. The absolute acceleration frequency response functions of the two base isolated buildings are shown in Figure 7 for the four cases. It is observed in this figure that adding the isolation layer reduces the resonant peak of the 5 Hz fixed-base structures to 0.5 Hz and 0.2 Hz for isolated building A and isolated building B, respectively. It is also noted that providing isolation reduces the acceleration responses by an order of magnitude (20 dB) above 1 Hz, which demonstrates the benefits of isolation. The magnitude of the resonant peaks, however, has increased from 28 dB for the fixed base structures to 34 dB for the isolated structures. This 6 dB increase corresponds to an increase by a factor of 2. This can be significant if, during a long-period long-duration earthquake, the resonance is excited.

To reduce this resonant peak, the damping in the isolation layer can be increased. The dotted lines in Figure 7 show the transfer functions for the isolated buildings with isolation-layer damping that corresponds to 10% of critical. The magnitudes of the resonant peaks are reduced by 12 dB relative to those with only 2% damping in the isolation layer. The 12 dB decrease corresponds to a reduction of ¼. However, it is known that increasing the damping of the isolation layer decreases the effect of the isolation, increasing the magnitude of the transfer functions at higher frequencies. This is observed here as an increase in the magnitude of the second resonant peak around 10 Hz, by nearly 15 dB, an increase of more than 5.5 times. The CCM provides a first-resonant peak reduction similar to adding isolation-layer damping but keeps the second resonant peak quite low. This example illustrates the tradeoff in traditional base isolation between a susceptibility to long period long duration earthquakes and the effectiveness of the isolation and the ability of the CCM to achieve both objectives in base isolation.

3. Conclusions

Simple analytical models are presented here to demonstrate, through a frequency domain analysis of the transfer functions from ground acceleration input to absolute acceleration output, that the connected control method can be applied to adjacent base-isolated buildings to provide reduction in the isolator resonant peaks while not increasing the attenuation of the responses. A numerical example is provided to demonstrate that the connected control method can protect isolated buildings from long-period long-duration earthquakes without affecting the performance of the isolation during higher frequency excitations. In addition to the demonstrated performance benefits, the application of the connected control method for adjacent base-isolated buildings has the added benefit of providing additional damping to both isolated buildings through the use of only one coupling damper and stiffness link. The use of fewer devices can decrease costs and maintenance.

4. Acknowledgements

This material is based upon work supported by the National Science Foundation under Grants No. 1344937 and 1446234. Any opinions, findings, and conclusions or recommendations expressed in this material are those of the authors and do not necessarily reflect the views of the National Science Foundation.

5. References

[1] Seto, K. (1994), Vibration Control Method for Flexible Structures Arranged in Parallel, Proc. First World Conference on Structural Control, Pasadena, CA, 2, FP3-62-71, August 1994.

[2] Asano, M., Yamano, Y., Yoshie, K., Koike, Y., Nakagawa, K., and Murata, T. (2003), Development of Active-Damping Bridges and Its Application to Triple High-Rise Buildings, JSME International Journal, Series C, Vol. 46, No. 3, 2003, 854-860.

[3] Klein, R.E., Cusano, C., and Stukel, J. (1972), Investigation of a Method to Stabilize Wind Induced Oscillations in Large Structures, Presented at 1972 ASME Winter Annual Meeting, New York, Paper No. 72-WA/AUT-H.

[4] Kunieda, M. (1976), Earthquake Prevent Design and Earthquake Proof Design for Structures, Journal of JSME, 79 (689), 86-91 (in Japanese).

[5] Paulay, T.: Moment Redistribution in Continuous Beam of Earthquake Resistant Multistory Reinforced Concrete Frames, Bulletin of New Zealand National Society for Engineering, Vol. 9, No. 4, 1976, pp. 205-212.

[6] Chopra, A. K.: Dynamics of Structures: Theory and Applications to Earthquake Engineering, Prentice Hall, New Jersey, USA, 1995.

[7] Yoshie, K., Koike, Y., Shiraki, H., Asano, M., and Yamano, Y. (2003), Active-damping bridges for buildings of Harumi Island Triton Square (Part 5, Control effect evaluation using performance records), Summaries of Technical Papers of Annual Meeting Architectural Institute of Japan, B-2 Structures, Structural Dynamics and Nuclear Power Plants, 717-718. (in Japanese)